

Mining Knowledge for HEp-2 Cell Image Classification

Petra Perner, Horst Perner, and Bernd Müller
Institute of Computer Vision and Applied Computer Sciences
Arno-Nitzsche-Str. 45
04277 Leipzig / Germany
Tel.: +49 341 8612273
Fax.: +49 341 8665 579
e-mail ibaiperner@aol.com <http://www.ibai-research.de>

* corresponding author: Petra Perner, Kurt-Eisner-Str. 81, 04275 Leipzig, Germany

Abstract. HEp-2 cells are used for the identification of antinuclear autoantibodies (ANA). They allow for recognition of over 30 different nuclear and cytoplasmic patterns, which are given by upwards of 100 different autoantibodies. The identification of the patterns has recently been done manually by a human inspecting the slides with a microscope. In this paper we present results on the analysis and classification of cells using image analysis and data mining techniques. Starting from a knowledge acquisition process with a human operator, we developed an image analysis and feature extraction algorithm. The collection of the data set was done based on an expert's image reading and based on the automatic extracted features. A data set containing 132 features for each entry was set up and given to a data mining algorithm to find out the relevant features among this large feature set and to construct the classification knowledge. The classifier was evaluated by cross validation. The results gave the expert new insights into the necessary features and the classification knowledge and show the feasibility of an automated inspection system.

Keywords: Image Mining, Data Mining, Medical Diagnosis, HEp-2 Cell Classification, Fluorescence Image Analysis, Decision Tree Induction

1 Introduction

In this paper we present results on the analysis and classification of cells, using image analysis and data-mining techniques. The kinds of cells that are considered in this application are HEp-2 cells, which are used for the identification of antinuclear autoantibodies (ANA) [5]. HEp-2 cells allow for recognition of over 30 different nuclear and cytoplasmic patterns, which are given by upwards of 100 different autoantibodies.

The identification of these patterns has up to now been done manually by a human inspecting the slides with the help of a microscope. The recent methodology for training a physician to perform this kind of diagnosis is that an experienced physician teaches the novices the decision-making strategy. The well-known problem in image interpretation "the difference

between showing and naming” makes this methodology hard to follow by novices. Even for an experienced physician it is often hard to decide the right class. The lacking automation of this technique has resulted in the development of an alternative technique based on chemical reactions (ELISA, [1]), which have not the discrimination power of the ANA testing. A more distinguishing and better understood vocabulary as a basis for decision-making and on the long-run an automatic image analysis and classification system would pave the way for a wider use of ANA testing. Recent work on the automation of ANA testing deals with the development of standardization methods [8] for staining of the patterns, but not with the automatic analysis and interpretation of these patterns.

We present our results on mining HEp-2 cell images. We follow the methodology described by Cios et al. [4], but extend them by the special needs concerned with image analysis and interpretation [12]. Starting from a knowledge-acquisition process with a human operator (see Sect. 2), we developed an automatic image analysis and a feature extraction algorithm for the objective measurement of image features, described in Sect. 3. A data set containing 132 features for each entry was set up (see Sect. 4) and given to our data mining tool to find out the relevant features among this large feature set and to construct the structure of the classifier, see Sect. 5. The classifier was evaluated by cross validation. The results show the feasibility of an automatic image-inspection system (see Sect. 6). The application of data mining helped to obtain knowledge about specific features of different classes, and to create models for decision-making. It also provided the discovery of an inherent non-evident link between classes and their imaging in the picture (see Sect. 7).

2 Understanding the domain and the data

The analysis of autoantibodies with indirect immunofluorescence is a key technology for the diagnosis of autoimmune diseases, i.e. diseases which are characterized by immunoreactivity of the body against its own molecular and structural components. Immunoglobulins against certain organs and – more importantly – against more general cellular structures such as nuclear and mitochondrial components are found.

The detection of such autoantibodies is of significant diagnostic value, because it allows not only to identify severe rheumatic diseases, but also helps to make predictions about their course and prognosis. The method of choice is fluorescence microscopy of freeze-cut HEp-2 cells, but this procedure is time-consuming and could hardly be automated in the past. Differentiation of immunoreactivity is generally done by two independently working

technicians or scientists with a high degree of experience and knowledge. The disadvantages of such a manual procedure are well known.

Recently the various HEp-2 cell images occurring in medical practice have been collected into a data base at the university hospital of Leipzig. The images were taken by a digital image-acquisition unit consisting of a microscope AXIOSKOP 2 from Carl Zeiss Jena, coupled with a color CCD camera Polariod DPC. The digitized images were of 8-bit photometric resolution for each color channel with a per pixel spatial resolution of 0.25 μm . Each image was stored as a color image on the hard disk of the PC but is transformed into a gray-level image without loss of information before being used for an automatic image analysis.

The scope of our work was to mine these images in order to determine the proper image features, which are basic for human reasoning and for the proper classification knowledge, so that it can be used in medical practice for diagnosis or for teaching novices. Besides that it should give us the basis for the development of an automatic image diagnosis system. An immunologist who is an expert in the field and acts as a specialist to other laboratories in case of diagnostically complex cases supported our experiment.

2.1 Brainstorming and Image Catalogue

First, we started with a brainstorming process that helped us to understand the expert's domain and to identify the basic pieces of knowledge. We could identify mainly four pieces of knowledge: 1. HEp-2 cell atlas [3], 2. the expert, 3. slide preparation and 4. a book describing the basic parts of a cell and their appearance.

Then the expert collected prototype images for each of the six classes appearing most frequently in his daily practice. The expert wrote down a natural-language description for each of these images. As a result we obtained an image catalogue having a prototype image for each class and associated to each image is a natural-language description of the expert (see Fig. 1). Each class has a symbolic class name and a class number consisting of 6 digits which is based on our own nomenclature.

+++ Insert Figure 1 +++

2.2 Interviewing Process

Based on these image descriptions we started our interviewing process. First, we only tried to understand the meaning of the expert description in terms of image features. We let him circle

the interesting object or object details in the image to understand the meaning of the description. After having done this, we went into a structured interviewing process asking for specific details such as: “Why do you think this object is *fine-speckled* and the other one is not. Please describe the difference between these two.” It helped us to verify the expert description and to make the object features more distinct.

Finally we could extract from the natural-language description the basic vocabulary (attributes and attribute values, see table 1) and associate the meaning to each attribute.

In a last step we reviewed the chosen attributes and the attribute values with the expert and found a common agreement on the chosen terms. The result was an attribute list which is the basis for the description of object details in the images. Furthermore, we identified the necessary set of feature descriptors which might be useful for the objective measurement of image features. In our case we found that describing the cells by their boundary and calculating the size and the contour of the cell might be appropriate. The different descriptors of the interphase cells and the nuclei of the cells might be sufficiently described by an intelligent and flexible texture descriptor. Therefore, we developed a texture descriptor based on the random sets [15][7].

+++ Insert Table 1 +++

3 Setting up the automatic Image Analysis and Feature Extraction Procedure

3.1 Image Analysis

The color image has been transformed into a gray level image. Histogram equalization was done to eliminate the influence of the different staining [13]. Automatic thresholding has been performed by the algorithm of Otsu [10]. The algorithm can localize the cells with their cytoplasmatic structure very well, but not the nuclear envelope itself. We then applied morphological filters like dilation and erosion to the image in order to get a binary mask for cutting out the cells from the image. Overlapping cells have not been considered for further analysis. They are eliminated based on a simple heuristic. Each object with an area bigger than 2 times the mean area was removed from the image. For each cell in the image are calculated the area A_{cell} and the features described in the next Section. Note that the image $f(x,y)$ considered for further calculation contains now only one cell.

3.2 Texture Feature Extraction

The texture model X is obtained by taking various realizations of compact random sets, implanting them in Poisson points in R^n , and taking the supremum. The functional moment $Q(B)$ of X , after Booleanization, is calculated as:

$$P(B \subset X^c) = Q(B) = \exp(-\theta \overline{Mes}(X \oplus \overset{\vee}{B})) \quad \forall B \in \kappa \quad (1)$$

where κ is the set of the compact random set of R^n , θ the density of the process and $\overline{Mes}(X \oplus \overset{\vee}{X})$ is an average measure that characterizes the geometric properties of the remaining set of objects after dilation. Relation (1) is the fundamental formula of the model. It completely characterizes the texture model. $Q(B)$ does not depend on the location of B , thus it is stationary. One can also provide that it is ergodic, thus we can peak out the measure for a specific portion of the space without referring to the particular portion of the space.

Formula 1 tells us that the texture model depends on two parameters:

1. on the density θ of the process and
2. a measure $\overline{Mes}(X \oplus \overset{\vee}{B})$ that characterizes the objects. In the 1-dimensional space it is the average length of the lines and in the 2-dimensional space $\overline{Mes}(X \oplus \overset{\vee}{B})$ is the average measure of the area and the perimeter of the objects under the assumption of convex shapes.

The 1-dimensional case has been studied by Garcia et al. [6]. We consider the 2-dimensional case and developed a proper texture descriptor. Suppose now that we have a texture image with 8 bit gray levels. Then we can consider the texture image as the superposition of various Boolean models, each of them taking a different gray level value on the scale from 0 to 255 for the objects within the bitplane.

To reduce the dimensionality of the resulting feature vector the gray levels ranging from 0 to 255 are now quantized into 12 intervals t . Each image $f(x,y)$ containing only a cell gets classified according to the gray level into t classes, with $t = \{0, 1, 2, \dots, 11\}$. For each class a binary image is calculated containing the value "1" for pixels with a gray level value falling into the gray level interval of class t and value "0" for all other pixels. The resulting bitplane $f(x,y,t)$ can now be considered as a realization of the Boolean model. The quantization of the

gray level into 12 intervals was done with equal distance. We call the image $f(x,y,t)$ in the following class image. Object labeling is done in the class images with the contour following method [9]. Afterwards, features from the bit-plane and from these objects are calculated.

The first one is the density of the class image t which is the number of pixels in the class image labeled by “1” divided by the area of the cell. If all pixels of a cell are labeled by “1” then the density is one. If no pixel in a cell is labeled then the density is zero. From the objects in the class image t the area, a simple shape factor, and the length of the contour are calculated. According to the model, not a single feature of each object is taken for classification, but the mean and the variance of each feature is calculated over all the objects in the class image t . We also calculate the frequency of the object size in each class image t . The list of features and their calculation is shown in table 2.

+++ Insert Table 2 +++

4 Collection of Image Descriptions into the Data Base

For our experiment we used a data set of 321 images. The data set contained 6 classes, each equally distributed. For each class we had 53 images. The gold standard for the class label was obtained by a test called ELISA. ELISA stands for enzyme linked immunosorbent assay. The expert displayed one after another each image from our database. He watched the images on display and described the image content on the basis of our attribute list and fed the attribute values as well as his decision about the class into the database. Therefore, the database contained a class label obtained by gold standard diagnosis and a class label given by the expert. That allowed us to compare the performance of the expert with the performance of the learnt classifier.

It is interesting to note that the expert could not make a decision about the class based on the inspection of a single cell. He was only confident in his decision when he found in the image some other cells called mitosis. This is a special type of cells implemented into the substrate to give the expert more confidence in his diagnosis. It often occurred that the expert could not decide which class label he should feed into the database. Therefore, the class label was extended to the label “no_decision”. However, he was forced to read the image features also in those cases where he could not make a decision about the class.

Finally we obtained a data base with 76.4 % of samples having a correct decision, 18 % of samples were the expert could not make a decision or made a wrong decision, and 5.6 % of

samples were he was not sure about the class and input two possibilities. We considered the two last cases as a false decision that gave us a portion of samples of 23.6%.

The same images were analyzed again by our image-analysis procedure and the features were automatically calculated by the program. The resulting values for these features are automatically fed into the database and stored together with the expert's image description into the database.

5 The Image Mining Experiment

The collected data set was then given to a decision tree induction program. Decision tree induction allows one to learn a set of rules and basic features necessary for decision-making in a diagnostic task. The induction process does not only act as a knowledge discovery process, it also works as a feature selector, discovering a subset of features from the whole set of features in the sample set that is the most relevant to the problem solution. A decision tree partitions the decision space recursively into sub-regions based on the sample set. In this way the decision tree recursively breaks down the complexity of the decision space. The outcome has a format, which naturally presents the cognitive strategy of the human decision-making process.

A decision tree consists of nodes and branches. Each node represents a single test or decision. In the case of a binary tree, the decision is either true or false. Geometrically the test describes a partition orthogonal to one of the coordinates of the decision space. The starting node is usually referred to as the root node. Depending on whether the result of a test is true or false, the tree will branch right or left to another node. Finally a terminal node is reached (sometimes referred to as a leaf), and a decision is made on the class assignment. Also non-binary decision trees are used. In these trees more than two branches may leave a node, but again only one branch may enter a node. For any tree all paths lead to a terminal node corresponding to a decision rule of the "IF-THEN" form that is a conjunction (AND) of various tests.

The main tasks during decision tree learning can be summarized as follow: attribute selection, attribute discretization, splitting, and pruning. We used for our experiment different decision tree induction methods. Each of these decision tree induction methods uses maximum entropy criteria [2] for the attribute selection during decision tree learning. Attribute discretization of numerical attributes during decision tree learning was done into binary intervals based on the entropy criteria and into more than 2 intervals based on the methods described in [11]. Thus, the resulting decision trees were binary trees and non-binary trees. Pruning was done based on

the reduced-error pruning technique [14]. The error rate was evaluated by leave-one-out cross-validation [16].

We carried out two experiments. First, we learnt a decision tree only based on the image readings by the expert, then we learnt a decision tree only based on the automatically calculated image features. The best results were obtained for the binary decision trees. The learnt non-binary decision trees did not perform as well as the binary trees on this kind of data. Therefore, we only report the results for the binary decision trees.

The resulting decision tree based on the expert's reading is shown in Figure 2 and in Figure 3 is shown the resulting decision tree based on the measured image features. It can be seen that from the whole set of features only a few features are selected for the decision trees. The performance of the expert as well as the error rate of the two learnt decision trees is shown in table 3.

+++ Insert Figure 2 +++

+++ Insert Figure 3 +++

+++ Insert Table 3 +++

6 Review

The performance of the human expert with an error rate of 23.6% was very poor (see table 3). The expert was often not able to make a decision when he did not see mitotic cells in the image. When the mitotic cells were absent in the image he could not decide the class. In that case he was not cooperative and did not read the image features. This behavior leads to the conclusion that he has not a very well built up understanding about the appearance of the image features nor does his decision making strategy really rely on a complex image interpretation strategy. The resulting decision tree based on the expert's reading shown in Figure 2 supports this observation. The decision-making strategy of the expert is only based on two image features, the `interphase_cells` and the `chromosomes`. This tree has an error rate of 16,6 %. However, for the "not_decided" samples in our database this tree could not be of any help since the expert did not read the image features in that case.

The tree based on the calculated image features shows an error rate of 25%. This performance is not as good as the performance of the expert, but the tree can also make a decision for the "not_decided" samples. We believe that the description of the different patterns of the cells by a texture descriptor is the right way to proceed. The Boolean model is flexible enough and we

believe that by further developing this texture model for our HEP-2 cell problem we will find better discriminating features which will lead to a better performance of the learnt tree.

Although the features calculated based on the Boolean model are of numerical type, they also provide us with some explanation capability for the decision making process. The sub tree shown on the right side of Figure 3 shows us for e.g. that the most important feature is *dens_0*. That means if there exist some objects in the *class image_0* which refers to low gray level (0-21 increments) the *class 500000* and partially the *class 200000* can be separated from all the other classes. That means a small number of dark spots inside the cell refer to *class 500000* and *class 200000*. This can be confirmed by the images shown in Figure 4. The discriminating feature between *class 500000* and *class 200000* is the standard deviation of the object contour in *class image_3*. Small contours of dark objects in class *image_3* refer to class 200000, whereas big contours refer to class 500000. This is also evident from the images shown in Figure 4.

It is interesting to note that not the features *fine_speckeld* or *fluorescent nucleoli* are the most discriminating features. The classifier based on the calculated image features takes other features and therefore leads to a new and deeper understanding of the problem.

+++ Insert Figure 4 +++

7 Using the discovered knowledge

The achieved results helped experts to understand their decision-making strategy better. It is evident now that the full spectrum of human visual reasoning is not exhausted for this inspection task. Instead of developing a sophisticated reasoning strategy by the physicians, the problem was given back to the developers and providers of the freeze cut HEP-2 cells. They implemented into the substrate special cells, for e.g. the so-called mitosis, as already mentioned in Sect. 4. Although mitosis give higher confidence in the decision, another problem still exists. These cells appear somewhere in the slides. It can only be guaranteed by the producers that a certain percentage of mitosis appear in each slide. It is highly likely that under the microscope the special cells are not visible since none of these cells lie in the chosen region of interest. Then the slide must be manually shifted under the microscope until a better region of interest is found. Besides that each company has a different strategy how to set up their substrate. A high percentage of mitosis in the substrate is a special feature for the products of one company. Another company has another special feature. However the real HEP-2 cells appear equally in the images.

Therefore our effort goes in two directions: 1. Setting up a more sophisticated image catalogue for teaching physicians and 2. Further development of our texture feature extractor. The image catalogue should explain in more details the different features and feature values of the vocabulary so that the expert is more certain in reading the image features although the mitosis is absent in the image. By doing that it should help the experts to understand their inspection problem better and to use a standard vocabulary with a clearly defined and commonly agreed meaning. The further development of our texture feature extractor should lead to better distinguishing features so that the performance of the classifier is improved. Besides that the explanation capability of the feature descriptor can be used for determining better symbolic features as the basis of the image catalogue.

The recent automatic image analysis and classification system based on the methods described in Section 3 and the classifier described in Section 5 is used as decision support system in medical practice. It serves as a test system and besides that helps the experts to better understand what is necessary for decision making.

8 Conclusion

In this paper we presented our results on mining HEp-2 cell images. The basis of our study was a large database of HEp-2 cells. We showed how the domain vocabulary could be elicited from the expert and how it can be used in order to get the image readings from the expert as a basis for the mining process. Besides that we showed how automatic image analysis and feature extraction could be used for an objective feature measurement. The feature descriptors are flexible enough to be used for other image analysis tasks and therefore they can be seen as one of the first algorithms in a basic set of feature extraction methods for a generic image mining system.

The mining experiment and the observations during the data mining process as well as the review of the results gave us a fundamental understanding of the basic features used by the expert for decision making and of his reasoning strategy. It could be shown that the visual concept behind the vocabulary is not clearly understood by the expert yet, since for a subset of samples the experts were unable to read the features from the images.

The mining experiment based on the objective feature measurements gave us new insights into the application. The performance of the resulting classifier is as good as the performance of the expert. The classifier can decide based on the image features of a single cell, while the expert needs mitosis to make a final decision.

The system based on the image analysis and feature extraction procedures and the learnt classifier is already in use as a decision support system at the university hospital Leipzig. Further developing the texture feature will do further improvement of the system.

Acknowledgement

The work presented in this paper is part of the project *LernBildZell* funded by the German Ministry of Economy.

References

- [1] Y. Abe, K. Kimura, A. Horiuchi, M. Miyake and Sh. Kimura, Improvement of ELISA sensitivity by allogeneric adsorption of polyclonal antibodies - a technical note for non-experts, *Clinica Chimica Acta*. 224(1994)103-105.
- [2] H.S. Baird and C.L. Mallows, Bounded-Error in Pre-classification Trees in: D. Dori and A. Bruckstein, eds., *Shape, Structure and Pattern Recognition* (World Scientific Publishing Inc., Singapore, 1995) 100-110.
- [3] A.R. Bradwell, R.P. Stokes, and G.D. Johnson, *Atlas of HEp-2 Patterns*, © AR Bradwell, 1995.
- [4] K.J. Cios, A. Teresinska, St. Konieczna, J. Potocka, and S. Sharma, Diagnosing Myocardial Perfusion SPECT Bull's-eye Maps - A Knowledge Discovery Approach, *IEEE Engineering in Medicine and Biology Magazine*, special issue on Medical Data Mining and Knowledge Discovery, 19 (4): 17-25.
- [5] K. Conrad, R.-L. Humbel, M. Meurer, Y. Shoenfeld, E. M. Tan, eds., *Autoantigens and Autoantibodies: Diagnostic Tools and Clues to Understanding Autoimmunity* (Pabst Science Publisher, Lengerich, Berlin, Riga, Rom, Wien, Zagreb, 2000).
- [6] P. Garcia, M. Petrou, and S. Kamata, The Use of the Boolean Model for Texture Analysis of Grey Images, *Computer Vision and Image Understanding*, 74 (1999) 227-235.
- [7] G. Matheron, *Random Sets and Integral Geometry* (J. Wiley & Sons Inc., New York London, 1975).

P. Perner, H. Perner, and B. Müller, Mining Knowledge for Hep-2 Cell Image Classification, *Journal Artificial Intelligence in Medicine*, 26 (2002), pp. 161-173

- [8] I. Nakabayashi et al, Evaluation of the Automatic Fluorescent Image Analysis, Image Titer, for Quantitative Analysis of Antinuclear Antibodies, *American Journal of Clinical Pathology*, 115 (2001), online <http://www.ajcp.com/>.
- [9] H. Niemann, *Pattern Analysis and Understanding* (Springer Verlag, Berlin Heideberg, 1990).
- [10] N. Otsu, A threshold selection method from gray-level histograms, *IEEE Trans. on Systems, Man, and Cybernetics*, 9 (1979) 38-52.
- [11] P. Perner and S. Trautzsch, Multi-Interval Discretization for Decision Tree Learning in: A. Amin, D. Dori, P. Pudil, and H. Freeman, eds., *Advances in Pattern Recognition*, LNCS 1451 (Springer Verlag, Heidelberg Berlin, 1998) 475-482.
- [12] P. Perner, A knowledge-based image inspection system for automatic defect recognition, classification, and process diagnosis, *International Journal on Machine Vision and Applications* 7 (1994) 135-147.
- [13] M. Petrou and P. Bosdogianni, *Image Processing: The Fundamentals* (John Wiley & Son Inc., Chichester New York Weinheim Brisbane Singapore Toronto, 1999).
- [14] J. R. Quinlain, Simplifying decision tree, *Intern. Journal on Man-Machine Studies* 27 (1987) 221-234.
- [15] D. Stoyan, W.S. Kendall, and J. Mecke, *Stochastic Geometry and Its Applications* (Akademie Verlag, Berlin, 1987).
- [16] S.M. Weiss and C.A. Kulikowski, *Computer Systems that Learn: Classification and Prediction Methods from Statistics, Neural Networks, Machine Learning, and Expert Systems* (Morgan Kaufmann, San Mateo, 1990).

| Attribute | Code | Attribute Values |
|------------------|-------------|-------------------------------------|
| Interphase Cells | 0 | Undefined |
| | 1 | Fine speckled |
| | 2 | homogeneous |
| | 3 | Coarse Speckled |
| | 4 | Dense fine speckled Fluorescence |
| | | |
| Nucleoli | 0 | Undefined |
| | 1 | Dark area |
| | 2 | fluorescence |
| | | |
| Background | 0 | Undefined |
| | 1 | Dark |
| | 2 | Fluorescence |
| | | |
| | | |
| Chromosomes | 0 | Undefined |
| | 1 | Fluorescence |
| | 2 | Dark |
| | | |
| | | |
| Cytoplasm | 0 | Undefined |
| | 1 | Speckled Fluorescence |
| | | |
| | | |
| Classes | 100 000 | Homogeneous |
| | 100 320 | Homogeneous fine speckled |
| | 200 000 | Nuclear |
| | 320 000 | Fine speckled |
| | 320 200 | Fine speckled nuclear |

Table 1 Attribute List

| Description | Name | Type | Formula |
|--|----------------|-----------|--|
| Area of the single cell | A_{cell} | numerical | $A_{cell} = \begin{cases} f(x, y, t) = 1 \text{ and object then } A_{cell} = A_{cell} + 1 \\ f(x, y, t) = 0 \text{ then } A_{cell} = A_{cell} \end{cases}$ |
| Density in class image t | $Dens_t$ | numerical | $Dens_t = \begin{cases} f(x, y, t) = 1 \text{ then } Dens_t = Dens_t + 1 / A \\ f(x, y, t) = 0 \text{ then } Dens_t = Dens_t \end{cases}$ |
| Number of objects | $Count_t$ | numerical | $n(t)$ |
| Mean area of objects in class image t | $Marea_t$ | numerical | $\bar{A}(t) = \frac{1}{n(t)} \sum_{i=1}^{n(t)} A_i(t)$ |
| Standard deviation of the area of the objects in class image t | $Staarea_t$ | numerical | $S(t) = \sqrt{\frac{1}{n(t)} \sum_{i=1}^{n(t)} (A_i(t) - \bar{A}(t))^2}$ |
| Mean shape factor for objects in class image t | $Form_t$ | numerical | $\bar{F}(t) = \frac{1}{n(t)} \sum_{i=1}^{n(t)} 10 \cdot \frac{A_i(t)}{u_i(t)}$ with $u_i(t)$ contour being the length of the i -th object in class image t . |
| The contour length of a single object is $u = l + \sqrt{2} \cdot m$ with l being the number of contour pixels having odd chain coding numbers and m being the number of contour pixels having even chain coding numbers. | | | |
| Mean contour length of objects in class image t | $Mlength_t$ | numerical | $\bar{u}(t) = \frac{1}{n(t)} \sum_{i=1}^{n(t)} u_i(t)$ |
| Standard deviation of the contour length of objects in class image t | $Stalength_t$ | numerical | $S(t) = \sqrt{\frac{1}{n(t)} \sum_{i=1}^{n(t)} (u_i(t) - \bar{u}(t))^2}$ |

Table 2 Image Feature List

| Method | Error Rate |
|--|------------|
| Expert | 23.6 % |
| Decision Tree based on Expert's Reading | 16.6 % |
| Decision Tree based on calculated Image Features | 25.0 % |

Table 3 Performance of Expert and Decision Trees

P. Perner, H. Perner, and B. Müller, Mining Knowledge for Hep-2 Cell Image Classification, Journal Artificial Intelligence in Medicine, 26 (2002), pp. 161-173

Fig. 1 Image Catalogue containing Class Name, Nomenclature, Sample Image and Expert's Description

Fig. 2 Decision Tree based on Expert's Reading

Fig. 3 Decision Tree based on Image Features

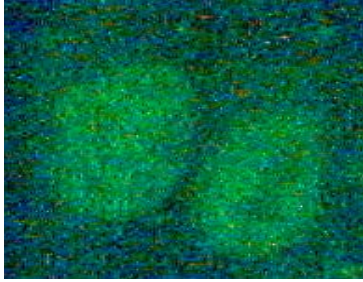
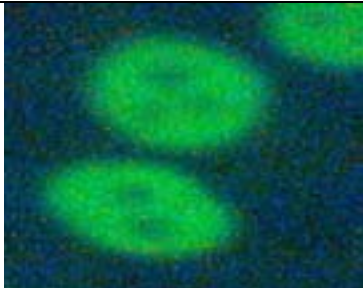
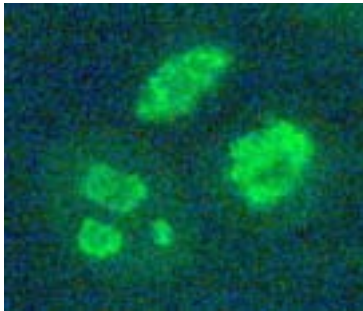
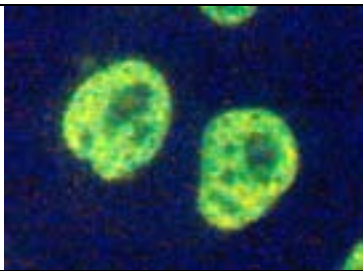
Fig. 4 Cells of Class 500000 and Class 200000

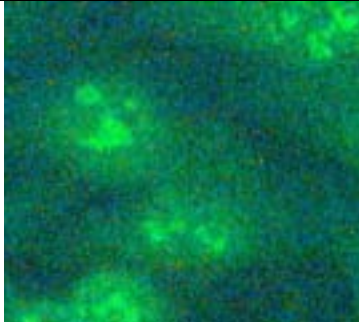
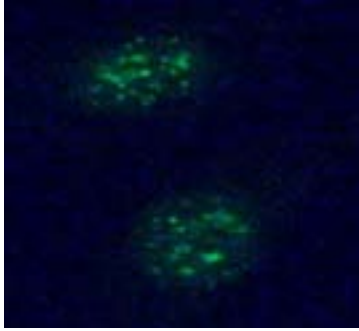
P. Perner, H. Perner, and B. Müller, Mining Knowledge for Hep-2 Cell Image Classification, Journal Artificial Intelligence in Medicine, 26 (2002), pp. 161-173

Table 1 Attribute List

Table 2 Image Feature List

Table 3 Performance of Expert and Decision Trees

| Class_Name | Nomenclature | Prototype Image | Description |
|-----------------------|--------------|---|---|
| Homogen | 100 000 |  | A uniform diffuse fluorescence of the entire nucleus of interphase cells. The surrounding cytoplasm is negative. |
| Homogen Fine Speckled | 100 320 |  | A uniform fine speckled fluorescence of the entire nucleus of interphase cells. |
| Nuclear | 200 000 |  | Smooth and uniform fluorescence of the nuclei Nuclei sometimes dark Chromosomes fluoresced weak up to extreme intensive |
| Fine Speckled | 320 000 |  | Fine to discrete speckled staining in a uniform distribution. |

| | | | |
|-----------------------|---------|--|---|
| Fine Speckled Nuclear | 320 200 |  | Dense fine speckled fluorescence Background diffuse fluorescent |
| Centromere | 500 000 |  | Nuclei weak uniform or fine granular, poor distinction from background |

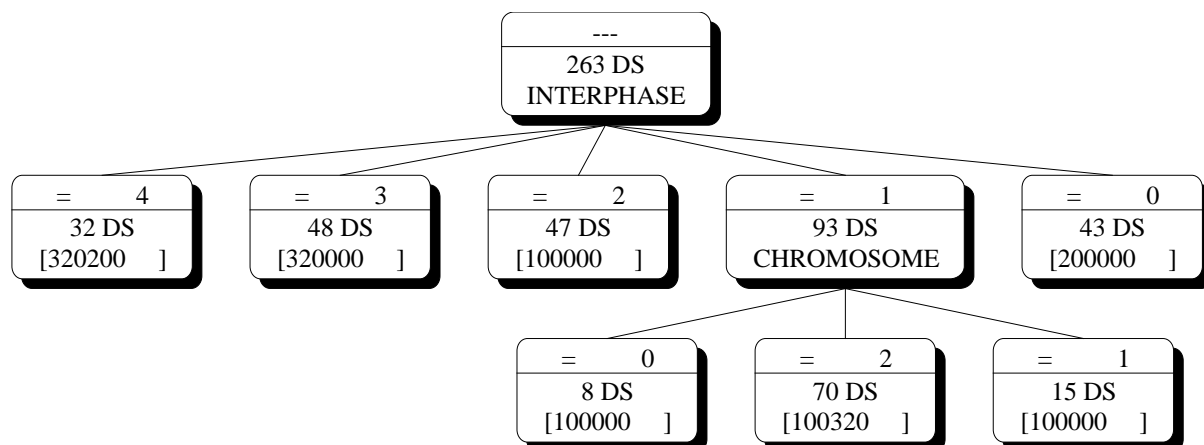


Fig. 2 Decision Tree based on Expert's Reading

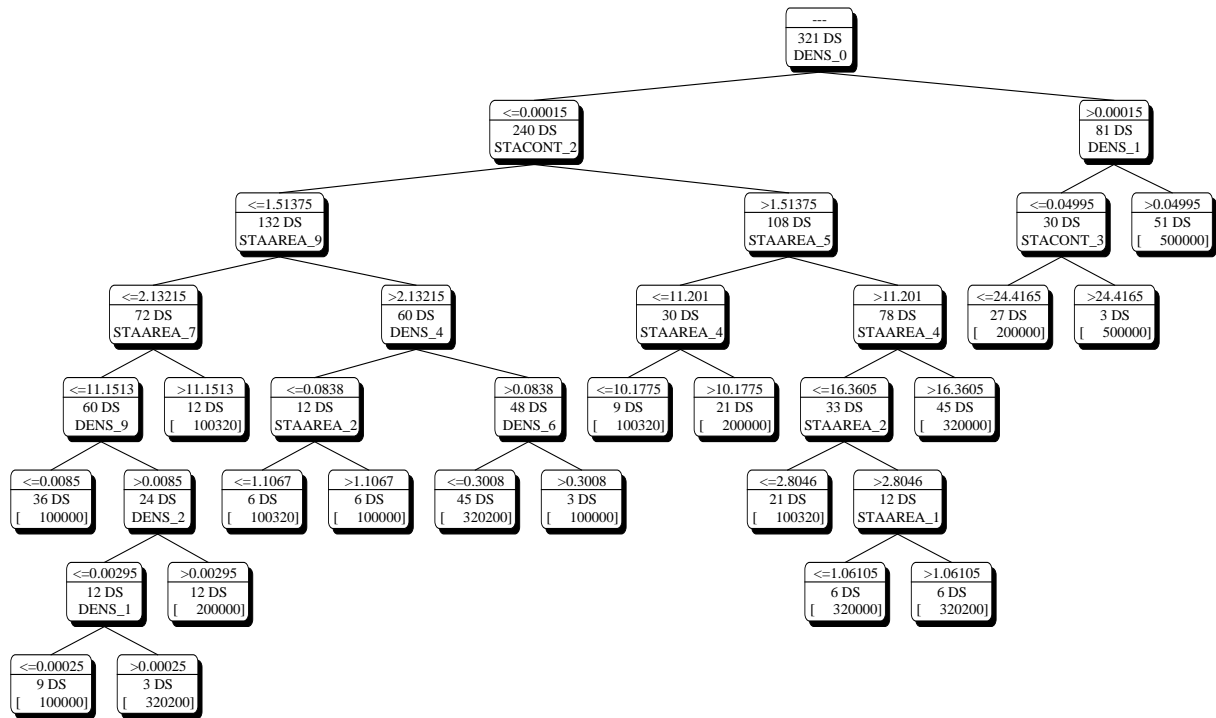


Fig. 3 Decision Tree based on Image Features



Fig. 4 Cells of Class 500000 and Class 200000

P. Perner, H. Perner, and B. Müller, Mining Knowledge for Hep-2 Cell Image Classification, Journal Artificial Intelligence in Medicine, 26 (2002), pp. 161-173